Food Chemistry: X 27 (2025) 102359

Contents lists available at ScienceDirect

Food Chemistry: X

journal homepage: www.sciencedirect.com/journal/food-chemistry-x

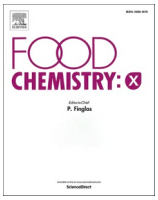

Roles of different polysaccharides on the structures of alginate-based Bigel beads and co-delivery of bioactives

Guangmin Liu [a,b], Yuxuan Wang [a,c], Jingyi Yang [c], Yaqin Wang [a,b,*], Hongju He [a,b,*], Like Mao [c]

[a] Institute of Agri-food Processing and Nutrition, Beijing Academy of Agriculture and Forestry Sciences, Beijing 100097, China
[b] Beijing Key Laboratory of Fruits and Vegetable Storage and Processing, Beijing 100097, China
[c] College of Food Science and Nutritional Engineering, China Agricultural University, Beijing 100083, China

ARTICLE INFO

Keywords:
Bigel
Bead
Curcumin
EGCG
Digestion
Release

ABSTRACT

Bigels are novel soft-solid materials, which attract increasing attentions in the food industry. In this study, bigel beads based on alginate hydrogel and monoglyceride oleogel were developed, and their structures were modified by adding various polysaccharides (pectin, carrageenan, chitosan, xanthan gum and konjac gum). The inclusion of polysaccharides generally increased bead size and decreased hardness, with chitosan reducing the shrinking rate and swelling ratio during simulated gastric-intestinal digestion. FTIR analysis confirmed no interactions between alginate hydrogel and monoglyceride oleogel, nor covalent bonds formation between alginate and the polysaccharides. The bigels were tested for simultaneously delivery of epigallocatechin gallate and curcumin, and the results showed that bead structures significantly influenced their release. Among all tested bigels, pectin and carrageenan beads exhibited the highest cumulative release in simulated intestinal fluid. The results suggested that polysaccharides effectively modified the physicochemical properties of alginate-based bigel beads, leading to adjustable release of the incorporated bioactives.

1. Introduction

Gels are semi-solid systems where the liquid phase is trapped by three-dimensional networks, and presented as soft materials. Basically, gels can be categorized into hydrogels and oleogels, depending on the polarity of the liquid phase (Mao, Lu, Cui, Song, & Gao, 2020). Bigels are novel biphasic systems, which contain both hydrogels and oleogels, and their structures can be oleogel-in-hydrogel (O/W), hydrogel-in-oleogel (W/O), and bi-continuous types. Bigels combine the advantages of both hydrogels and oleogels, and thus are attracting increasing attention in recent years (Shakeel et al., 2019). Generally, bigels have good spreadability, thermal stability, cooling and moisturizing effects, and they are also able to deliver hydrophilic and lipophilic bioactives simultaneously (Zheng, Mao, Cui, Liu, & Gao, 2020). Currently, bigels are mainly studied for drug delivery and cosmetic applications, with a few studies in the food field (Yang, Song, Miao, Gao, & Mao, 2024). On the other hand, gels can be turned into beads, which may have novel applications. Gel beads can be easily dispersed in food matrices due to their low density, and allow better control of the release of incorporated bioactives during digestion because of the high surface area (Lin, Kelly, & Miao, 2022). However, only very minor attention was paid on bigel beads (Yang et al., 2024). A previous study by the authors' group developed bigel beads with good sphericity and physical stability, and revealed that the beads with higher oleogel content had lower shrinkage ratio and swelling level (Yang et al., 2024). It was still unknown the role of the aqueous phase (i.e., the hydrogel) in the properties and functions of the bigel beads.

Alginate is the most widely used biopolymer for the preparation of gel beads, as it gels quickly in the presence of divalent cations, particularly Ca^{2+} ions. Ca^{2+} ions selectively bind to the G sequences of alginate to form an "egg-box" structure and further develop into thermal-stable three-dimensional networks (Cao, Lu, Mata, Nishinari, & Fang, 2020). However, alginate gel networks are highly porous and permeable, leading to quick loss of entrapped substances during gelation and storage. Dashevsky (1998) reported that the gelation of 1 % sodium alginate was accompanied by a loss of 44 % of water and 36 % of lactase enzyme. Therefore, modification in the composition of the aqueous phase has been proposed to overcome these limitations (Belščak-Cvitanović et al., 2015). Addition of other biopolymers (e.g., polysaccharides and proteins) to modify the gelation behaviors of sodium alginate (forming composite gels) was proved to be effective in modulating the structures and functions of bulk alginate gels (Ramdhan,

* Corresponding authors at: Institute of Agri-food Processing and Nutrition, Beijing Academy of Agriculture and Forestry Sciences, Beijing 100097, China.
E-mail addresses: wangyaqin@iapn.org.cn (Y. Wang), hehongju@iapn.org.cn (H. He).

https://doi.org/10.1016/j.fochx.2025.102359
Received 3 December 2024; Received in revised form 7 March 2025; Accepted 7 March 2025
Available online 10 March 2025

Ching, Prakash, & Bhandari, 2020).

Generally, three types of composite gels can be formed: complex gels, mixed gels and filled gels, and they have different structures and applications. In composite gels, alginate could interact with oppositely charged biopolymers and form three dimensional networks. In mixed gels, alginate and the additional biopolymer could develop discrete gels without any interaction or with just poor physical interactions. Filled-alginate gels referred to the gels with non-gelling ingredients. Alterations in matrix composition and internal structures (e.g., porosity) in different composite gels could significantly modify the roles of the gels to retain, protect and release the entrapped bioactives (Mao et al., 2020). In previous studies, pectin, chitosan, carrageenan, and xanthan gum were used to modify the properties of alginate gels (Ramdhan et al., 2020). Low methoxyl (LM) pectin could form ionic gels in the presence of Ca^{2+}, thereby generated mixed gels with alginate, leading to enhanced mechanical strength and stability of the gel beads. Wu et al. (2022) found that alginate composite gels with a proper pectin-alginate ratio could remarkably improve the encapsulation efficiency and loading capacity of bioactive compounds. Carrageenan could also be cross-linked with alginate upon suitable triggers to form complex gels (Al-Faken, Al-Subaie, EL-Ghoul, & Hamden, 2024). Li (2019) reported that the encapsulation efficiency of immunoglobulin Y (IgY) in carrageenan-alginate gel beads reached 63.01 %, and the retention rate of IgY activity after gastric digestion was increased by 35.41 %. Chitosan was able to interact with the negatively charged carboxylate groups of alginate and form mixed gels, resulting in gel beads with reduced porosity and higher compactness. Furthermore, chitosan could hinder the solubilization of alginate gel at alkaline pH. Zhu et al. (2023) prepared chitosan-coated hydrogel beads, and the chitosan layer did not swell in simulated gastric fluid. As a result, water molecules in the medium had poor permeability to the interior of the gel beads. Xanthan gum and konjac gum could interact with alginate, and the interaction degree was highly affected by the concentration of calcium ions and the mixing ratio of the two biopolymers (Cofelice, Messia, Marconi, Cuomo, & Lopez, 2023). However, very little information was available on the roles of polysaccharides on bigels structures and functionality.

In this study, novel bigel beads were developed, and their structures were modified to better accommodate bioactives. It was hypothesized that different polysaccharides in the water phase would affect the structures of both the water phase and oil phase, leading to different release behavior of the incorporated hydrophilic and hydrophobic bioactives from the beads. Two popular bioactives, one lipophilic (curcumin), one hydrophilic (epigallocatechin gallate, EGCG), were tested as model bioactives. In fact, some studies revealed that curcumin and EGCG had synergistic health effects (Chung & Vadgama, 2015). The objective of this work was to develop bigel beads based on alginate and different polysaccharides, i.e., pectin, carrageenan, chitosan, xanthan gum and konjac gum for enhanced stability and function of alginate gel beads. The composite bigel beads were systematically characterized, including size, sphericity, shrinkage ratio and rheological behaviors. Curcumin and EGCG were later incorporated simultaneously within the gel beads, and their release kinetics in an in vitro test were investigated.

2. Materials and methods

2.1. Materials

Sodium alginate (M:G = 1:1, viscosity 200–550 mPa.s), calcium chloride (anhydrous), chitosan (degree of deacetylation~90 %, MW ~ 100,000 Da), potassium thiocyanide, dipotassium hydrogen phosphate (99.5 % purity) and potassium dihydrogen phosphate (99.5 % purity) were bought from Shanghai Macklin Biochemical Co., Ltd. (Shanghai, China). Apple Pectin (degree of esterification 27 %) and κ-Carrageenan (>90 % purity) were the products of Azelis Co., Ltd. (Shanghai, China). Konjac gum (viscosity>15,000 mpa.s) was purchased from Shanghai Yuanye Bio-Technology Co., Ltd. (Shanghai, China). Monoglycerides (GMS, DIMODAN®) and xanthan gum (MW ~ 241 kDa) were bought from Danisco (China) Co., Ltd., (Shanghai, China). Corn oil (Changshouhua) was bought from a local store. Tween 20 (TW) (HLB = 16.7), curcumin (98 % purity), and trichloromethane were the products of Sinopharm Chemical Reagent Co., Ltd. (Shanghai, China). EGCG was kindly offered by BSZH Scientific Inc. (Beijing, China). Nile red, mucin, pepsin, pancreatin, pancreatic lipase, bile salt and iron (II) chloride tetrahydrate (98 % purity) were obtained from Sigma-Aldrich (St. Louis, U.S.A.). All other chemical reagents were analytical grade.

2.2. Preparation of bigels

The preparation of bigels followed a method described previously (Yang et al., 2024). The water phase was obtained by dispersing sodium alginate in distilled water and stirring at room temperature (25 °C) until completely dissolved. The solution was stood overnight to remove air bubbles. Carrageenan (κ-ca), konjac gum (KGM), xanthan gum (XAN) and pectin (P) solutions were prepared with certain concentration. Carrageenan and konjac gum were stirred at 60 °C until completely dissolved. Sodium alginate (SA) solutions were mixed separately with κ-ca, KGM, XAN and P solutions to achieve final concentrations of 0.9 % (*w*/w) for sodium alginate and 0.6 % (w/w) for polysaccharides. When no other polysaccharide was added, SA with a concentration of 1.5 % (w/w) was included in the water phase. TW-20 (0.15 % w/w) which was served as surfactant was added into the aqueous solution. The oil phase was prepared by mixing GMS (10 % w/w) and corn oil at 80 °C, and placed at 4 °C for 0.5 h to form oleogels. EGCG (0.3 % w/w) was dissolved in the water phase at 25 °C, and curcumin (0.20 % w/w) was dispersed in the oil phase at 140 °C. To minimize curcumin degradation and oil oxidation, the oil solution was cooled immediately following curcumin dissolution. To obtain bigels, the oil phase and the water phase were mixed at a ratio of 2:8 using a magnetic stirrer (Ultra-Turrax, IKA, Germany) until homogenous mixtures were generated.

2.3. Preparation of bigel beads

The preparation of bigel beads followed a method described previously (Yang et al., 2024). The emulsions prepared in 2.2 were dropped through a syringe (0.7 mm i. d.) into 3 % (*w*/w) calcium chloride solution using a peristaltic pump (BT301F, Leadfluid, Baoding, China) at a rate of 0.15 mL/S. After 30 min of bead formation, the beads were collected by filtration and washed with distilled water. The beads were stored in distilled water at room temperature, and the analysis was finished within 3 h. Bigel beads with different polysaccharide fractions in the emulsions were termed SA, κ-ca, P, KGM and XAN, respectively. As for chitosan-coated beads, chitosan was dissolved in an acetic acid solution using a magnetic stirrer in advance. 3 % (w/w) $CaCl_2$ was added to the solution, and the concentration of chitosan in the final solution was 0.6 % (w/w). The formation of chitosan-coated beads is the same as that of other polysaccharide groups. The chitosan-coated beads were coded as CHI.

2.4. Rheological characterization

The shear viscosity of the emulsion was determined by rotational rheometer HAAKE MARS iQ AIR (Thermo Fisher Scientific, USA) adopting a parallel plates geometry (diameter = 40 mm, gap 1.0 ± 0.1 mm). The shear rate ranged from 0.01 to 100 s^{-1}, and all samples were tested at 20 °C.

2.5. Microstructural observation

The surface morphology of microgel beads was observed by SU8020 scanning electron microscope (SEM, Hitachi Co, Ltd. Tokyo). The freeze-dried beads were coated with gold and then observed under 15 kV acceleration potential.

The microstructure of the microgel beads was carried out by confocal laser scanning microscopy (CLSM). The beads were cut into transparent slices (~0.5 mm) and stained by Nile red ethanol solution (0.01 %, *w/w*). Afterwards, the stained samples were placed under the inverted confocal laser scanning microscope (Zeiss LSM880, Zeiss, Inc., Germany). The excitation light was set to 488 nm.

2.6. Shrinking rate

Determination of shrinking rate followed a method described in a previous study (Zhang, Yang, Li, Gao, & Mao., 2025). The shrinking rate was calculated using eq. (1):

$$\textit{Shrinking rate}\ (\%) = \left(1 - \frac{W_1}{W_0}\right) \times 100 \quad (1)$$

Where W_1 was the weight of the fresh bigel beads after gelation and W_0 was the emulsions used corresponded before gelation.

2.7. Swelling study

The swelling behavior of the fresh bigel beads was determined in distilled water (Yang et al., 2024). Fresh beads of accurate weight were immersed in 20 mL distilled water and periodically taken out from the medium. The water on the surface of the beads was then removed using filter paper, and the beads were weighed. The swelling ratio of bigel beads was calculated according to eq. (2):

$$\text{Swelling ratio}\ (\%) = \frac{W_t}{W_0} \times 100 \quad (2)$$

Where W_t was the weight of the swollen beads at time t and W_0 was the initial weight of the beads.

2.8. Determination of textural properties

The hardness of spherical beads was evaluated by a CT3 texture analyzer ((BROOKFIELD, Middleboro, Massachusetts, USA) coupled with a TA/0.5 cylindrical plunger at room temperature. A compression test was carried out with a test speed of 0.5 mm/s, post-test speed of 0.5 mm/s, contact force of 0.05 N, and compression deformation of 30 % (Cui et al., 2022).

The hardness of the beads was determined before and after swelling in SSF and SGF and the rate of change was calculated using eq. (3):

$$\textit{Hardness change ratio} = \frac{m_2 - m_1}{m_1} \quad (3)$$

Where m_1 was the hardness of beads before swelling in SSF and SGF, and m_2 was the hardness after swelling.

2.9. Fourier transform-infrared (FTIR) spectroscopy analysis

The FTIR analysis of the beads was determined by potassium bromide pellet using the Nicolet iS10 spectrometer (Thermo Fisher Scientific, Waltham, MA, USA). The analysis was carried out with a spectrum from 400 to 4000 cm^{-1}, a resolution of 4 cm^{-1} and 32 scans.

2.10. In vitro swelling study

In vitro swelling study was conducted followed a previous method with some modifications (Li et al., 2021). To eliminate the effects of enzymes but focus on the effects of salts, the swelling capacity of the beads was determined in enzyme-free simulated gastric fluid (ESGF, 0.68 % K_2HPO_4, 0.8775 % NaCl, pH 3.0) and enzyme-free simulated intestinal fluid (ESIF, 0.68 % K_2HPO_4, 0.8775 % NaCl, pH 7.0). Beads of accurate weight were immersed in ESGF or ESIF in an orbit shaker (37 °C) with stirring at 100 rpm (DSHZ-300, Taichang Experimental Instrument Co. Ltd., Jiangsu, China). At regular time intervals, beads were separated from the medium, and water on the surface was removed by filter paper. Swelling ratios with respect to time in ESGF and ESIF were calculated using eq. (2).

2.11. In vitro release profile

In vitro release experiment was carried out by the methods of Lin, Kelly, Maidannyk, and Miao (2021) with some modifications. Digestion of the beads and the release of EGCG and curcumin were tested in simulated oral, gastric and intestinal fluids. Simulated saliva fluid (SSF), simulated gastric fluid (SGF) and simulated intestinal fluid (SIF) were prepared according to Table S1 (supplementary data).

Oral phase: Bigel beads (~5 g) were mixed with 10 mL SSF and placed in an orbit shaker (37 °C) at 100 rpm for 2 min.

Gastric phase: After oral digestion, 10 mL SGF was added to the mixture and placed in an orbit shaker (37 °C) at 100 rpm for 6 h. Samples were collected at a certain interval during the digestion. After each sampling, 1.0 M NaOH was added and the pH was adjusted to 7.5 to terminate the hydrolysis of pepsin in the collected samples.

Intestinal phase: After gastric digestion, 30 mL SIF was added to the mixture and placed in an orbit shaker (37 °C) at 100 rpm for 5 h. Samples were collected at an interval of 30 min for the first 2 h, followed by intervals of 1 h and 2 h. After each sampling, the collected sample was placed in an ice water bath to terminate digestion.

The collected samples were centrifuged at 10,000 rpm for 10 min to collect 1 mL of supernatant. The supernatants were mixed with trichloromethane and vortexed for 2 min, and then centrifuged at 10,000 rpm for 2 min. The organic phase was collected and extracted three times, and then diluted with trichloromethane, followed by measurement of the absorbance of the supernatant at 416 nm using an 1800 UV–visible spectrophotometer (Shimadzu, Japan). The concentration of curcumin was calculated using the standard curve. After the extraction of curcumin, the remaining water phase was mixed with an appropriate amount of deionized water and centrifuged at 10,000 rpm for 2 min. The extract was collected and diluted with deionized water. Subsequently, absorbance was measured at 273 nm. The concentration of EGCG was calculated using the standard curve. Release amounts of curcumin and EGCG during digestion process were calculated with the following eq. (4):

$$\textit{Release amount of curcumin} \Big/ \textit{EGCG} = \frac{C_t}{C_0} \quad (4)$$

Where C_0 was the initial content of curcumin or EGCG in beads, and C_t was the content of curcumin or EGCG at time t during digestion process.

The release mechanisms of curcumin and EGCG were evaluated with the following models:

$$\text{Zero} - \text{order kinetics model} : Q_t = kt + Q_0 \quad (5)$$

$$\text{First} - \text{order kinetics model} : lnQ_t = lnQ_0 + kt \quad (6)$$

$$\text{Hixson} - \text{Crowell model} : Q_0^{1/3} - Q_t^{1/3} = kt \quad (7)$$

$$\text{Higuchi kinetics model} : Q_t = k\sqrt{t} \quad (8)$$

$$\text{Korsmeyer} - \text{Peppas model} : Q_t = kt^n \quad (9)$$

Where Q_t and Q_0 were the amounts of curcumin or EGCG at time t and 0, k were the release kinetic constants of different models, and n was the release exponent.

2.12. Statistical analysis

The experiments were repeated at least three times and the results were analyzed statistically using Excel and Origin 2018 software. The values were expressed as means±SD. Data were analyzed by a one-way

analysis of variance (ANOVA) with SPSS 23 software (IBM Corporation, USA). *P*-values of 0.05 or less were considered to be significant.

3. Results and discussion

3.1. Rheological properties of bigel emulsions

Viscosity of the emulsions before the formation of bigel beads was first characterized by rheological tests (Fig. 1). With the increase in shear rate, viscosity of all the emulsions was decreased, exhibiting a shear thinning behavior. Similar results were also reported in a previous study, and the viscosity of the emulsions could be affected by the emulsifier at the interface, and the polysaccharides in the water phase (Zhang et al., 2025; Lin et al., 2024.). At the same shear rate of 0.1 s^{-1}, the emulsion containing κ-ca or KGM presented the highest viscosity, which was nearly six times higher than that of the bigel emulsion without any additional polysaccharide. As the concentration of alginate in CHI was the lowest, it showed the lowest viscosity. The viscosity of XAN and P were 73.01 Pa·s and 40.50 Pa·s, respectively.

3.2. Morphology and microstructures of bigel beads

Fig. 2A showed the macroscopic images of the bigel beads. All the beads were pale yellow in color, but the sphericity and particle size varied. The SA and P beads had regularly spherical shape, while in the XAN and KGM beads, there were many oval-shaped beads. This could be explained by the weak ability of konjac and xanthan gum to cross-link with Ca^{2+} to form gels, as well as the possibility of phase separation during gelation, which resulted in a decrease in the homogeneity of the structures (Zhang et al., 2013). In the CHI beads, there were some tear-shaped beads due to the low viscosity of the bigel emulsion and the high viscosity of the gelling bath. During the gelation process, the immersing depth of the droplets in the gelling bath was reduced and the collision force of the droplets against the bath surface was enhanced, which contributed to deformation of the beads (Lee, Ravindra, & Chan, 2013). The size of all the beads ranged from 1.88 to 2.46 mm, with a size order of XAN > κ-ca > P > KGM, SA > CHI (Fig. 2A). Previous studies have demonstrated that the size of beads was highly affected by the viscosity, and an appropriate increase in the viscosity of the system aided in the formation of beads with higher sphericity and larger size (Lee et al., 2013).

SEM images of bigel beads were given in Fig. 2B, and it was seen that all samples had spherical shapes and rugged surface. After freeze drying, structural collapse and shrinking took place at the surface of the alginate gel beads (without oleogel), resulting in irregular structures. All bigel beads had much smoother surface, suggesting that oleogel filling could resist structural collapse during freeze drying. The overall structure of the bigel beads was comparable to that of alginate based emulsion gel beads in the study by Murata, Sasaki, Miyamoto, and Kawashima (2000). The CHI beads displayed a smoother surface and less concave features, which could be associated with the polyelectrolyte complexes formed by ionic interactions between the amino groups in chitosan and the carboxyl residues of alginate. Similar results were also observed in previous study (Liu, 2018).

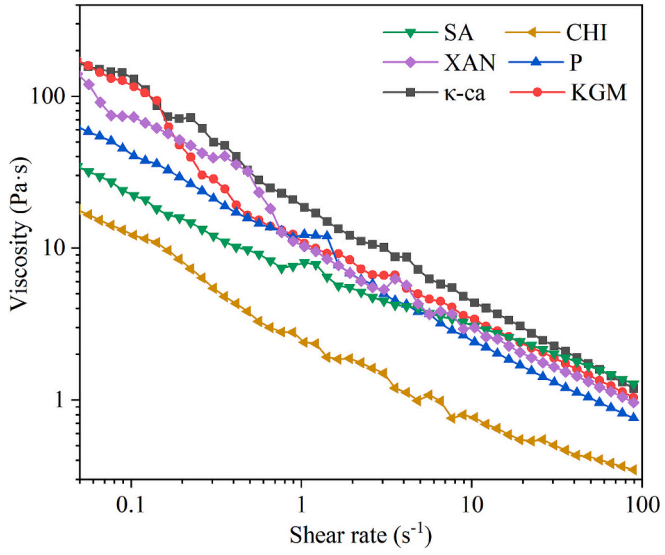

Fig. 1. Viscosity of emulsions before gelation.

3.3. Physical properties of the bigel beads

The formation of alginate gel was accompanied by shrinkage, and the shrinking rate was influenced by gel strength, filler content and structures, as well as the interaction between the filler and the continuous phase. All bigel beads shrank at a substantially slower pace than pure alginate hydrogel beads (~64.34 %), indicating that the oleogel filling remarkably hindered gel shrinkage (Table 1). The inclusion of various polysaccharides, except chitosan, reduced the shrinkage of SA beads to different degrees ($p > 0.05$). The shrinking rate of SA beads (42.67 %) was lower than that of CHI beads (50.51 %), implying that SA beads had a denser gel structure and higher gel strength. This result was in agreement with the research on Pickering emulsion based gel beads (Wu, Li, Xia, & Li, 2022). κ-Ca and XAN beads exhibited the lowest shrinking rates (32.63 % and 35.23 %). This finding was in line with the variation in particle size, and higher shrinking rates generally contributed to the reduction in bead size. The swelling ratio of bigel beads stored in deionized water was determined to assess their stability during equilibration. As can be seen from Table 1, all beads showed similar swelling behavior: the swelling ratio was increased to ~100 % after 1 day of storage, and all samples shrank after 2 days. Likewise, xanthan gum and κ-carrageenan were found to be effective in resisting the shrinkage of the beads, thus improving their stability. The pores of the alginate network in XAN beads could not be well recognized, which could be attributed the interactions between xanthan and alginate (Cofelice et al., 2023). Such interactions led to a more compact network structure and less shrinkage during gel equilibration. Alginate and κ-carrageenan could create a crosslinking network through hydrogen bonding and ionic interactions, which minimized the intermolecular spacing between alginate and κ-carrageenan, and led to a more compact network structures with higher resilience to swelling and shrinkage.

The textural properties of alginate gel beads were mainly dependent on alginate concentration and the strength of cross-linked gel networks (Aw et al., 2023). The bigel beads hardness of different samples followed the order of SA, XAN > KGM > κ-ca, CHI > P, but the difference was quite small (Table 1). For the CHI beads, CHI was dissolved in the $CaCl_2$ solution first, and not all CHI could cover the surface of the gel beads. Therefore, the total concentration of polysaccharide in the CHI beads would be much lower, leading to limited mechanical strength and thus lower hardness. The addition of P (0.20 N) and κ-ca (0.21 N) reduced their hardness, which was due to the fact that the networks formed by the secondary polysaccharide and Ca^{2+} were weaker than those formed by alginate and Ca^{2+} (Qi, Simsek, Chen, & Rao, 2020). Bigel beads with higher textural properties were more considerable as an oral delivery system for their higher resistance to the contraction force of gastrointestinal digestion.

3.4. FTIR analysis

FTIR spectra of the bigel beads were obtained to understand the impact of polysaccharide type on the structures of bigel beads (Fig. 3). The peak shape of the bigels was similar to that of the oil phase, which was mainly attributed to the higher proportion of oleogel in the bigel beads. The broad spectrum at ~3472 cm^{-1} suggested O—H stretching,

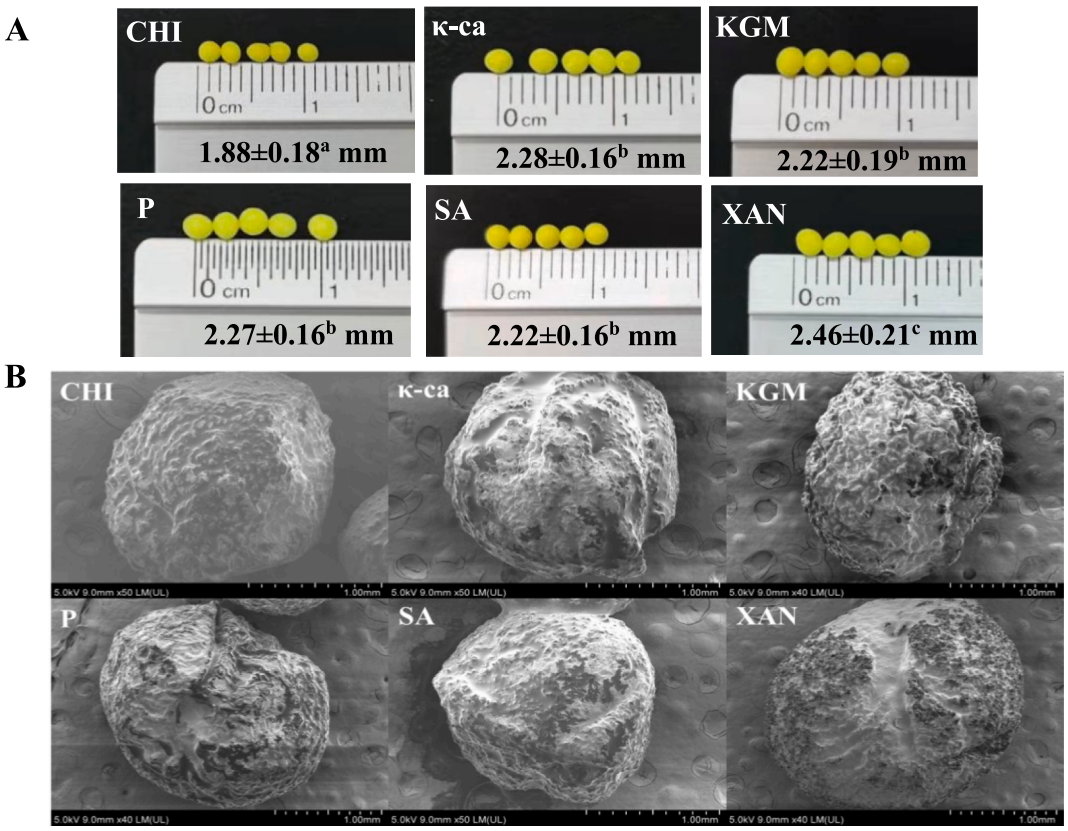

Fig. 2. Macroscopic images (A) and SEM images (B) of bigel beads with different types of polysaccharides.

Table 1
Physicochemical properties of bigel beads with different types of polysaccharides.

Samples	Shrinking rate (%)	Swelling ratio in deionized water (%)		Hardness (N)	Hardness after swelling in SSF and SGF (N)
		1 day	2 day		
XAN	35.23 ± 1.05^{b}	100.82 ± 1.11^{ab}	97.20 ± 1.30^{a}	0.24 ± 0.02^{a}	0.16 ± 0.02^{c}
SA	42.67 ± 1.58^{d}	98.65 ± 1.19^{b}	93.83 ± 1.11^{b}	0.24 ± 0.01^{a}	0.27 ± 0.02^{a}
P	39.38 ± 0.43^{c}	100.07 ± 1.63^{ab}	94.07 ± 1.16^{b}	0.20 ± 0.02^{b}	0.19 ± 0.02^{b}
KGM	41.21 ± 0.59^{cd}	98.35 ± 0.25^{b}	93.94 ± 0.93^{b}	0.22 ± 0.02^{b}	0.19 ± 0.08^{b}
κ-ca	32.63 ± 0.19^{a}	102.24 ± 0.39^{a}	96.41 ± 0.62^{a}	0.21 ± 0.01^{b}	0.10 ± 0.02^{d}
CHI	50.51 ± 1.25^{e}	99.67 ± 1.43^{b}	93.66 ± 1.44^{b}	0.21 ± 0.02^{b}	0.19 ± 0.02^{b}

Note: a-e means within the same column of each treatment with different superscript letters are significantly different at $p < 0.05$.

corresponding to inner- and intra-molecular hydrogen bonds (Belščak-Cvitanović et al., 2015). The stretching bands of C—H and C═H at ~2927 cm^{-1}, ~2853 cm^{-1} and ~ 1465 cm^{-1} corresponded to saturated and unsaturated fatty acyl chains of the oil phase (Goodacre & Anklam, 2001). Vibration of the C═O band was also observed at ~1746 cm^{-1} and ~ 1165 cm^{-1}. There were no new peaks or drastic shifting observed in the spectra of bigel beads. The findings suggested that there were no interactions between alginate hydrogel and GMS oleogel, nor any covalent bonds formed between alginate and polysaccharides.

3.5. Swelling behaviors of the beads during digestion

The influence of polysaccharide type on the swelling behavior of bigel beads during gastrointestinal digestion was determined. Fig. 4A presented the morphology of bigel beads after 6 h of digestion in ESGF. The structure of bigel beads remained almost intact after gastric digestion and all emerged at the top of the centrifuge tubes, whereas pure hydrogel beads moved to the bottom of the tubes (HY). It was agreed that calcium alginate beads shrink under acidic gastric conditions because protonation of the carboxyl groups means the alginate chains can get closer together, which worked to maintain the structures of the beads (Lin et al., 2024). The movement of the beads could be explained by the floatability of the bigel beads due to the low density of the oleogel (Kour et al., 2022). The floatability of the beads could prevent them from gastric emptying, thereby prolonging the residence and release time of the substance in the stomach. It was also observed that only a small amount of curcumin was released in ESGF, favoring the retention of fat-soluble substances in the stomach.

As shown in Fig. 4B, with the extension of ESIF digestion, all samples displayed a considerable rise in particle size at the beginning, and the gel structures gradually blurred from the edge, eventually disintegrated. There was no oil release observed, implying that the solubilization of the system was mainly related to the aqueous phase in the absence of digestive enzymes.

The distinct swelling behaviors of bigel beads presented in ESGF and ESIF were attributed to the pH responsiveness of alginate. When in ESGF (pH = 3), the swelling ratios of all samples grew slowly and remained consistently low, indicating their strong resistance to swelling as a result of hydrogen bonding between protonated carboxyl groups in alginate (Berninger, Mitter, & Preininger, 2016). At the same time, Na^{+} in the medium underwent ion exchange with Ca^{2+} at the mannuronic acid group of the alginate molecules. Since Na^{+} was not able to bind -COO^{-} from the mannuronic acid group completely, the increase in the number of -COO^{-} facilitated electrostatic repulsion between the alginate chains (Lin et al., 2024). The results could be responsible for the dramatic increase in osmotic pressure and water uptake of the bigel beads. It was

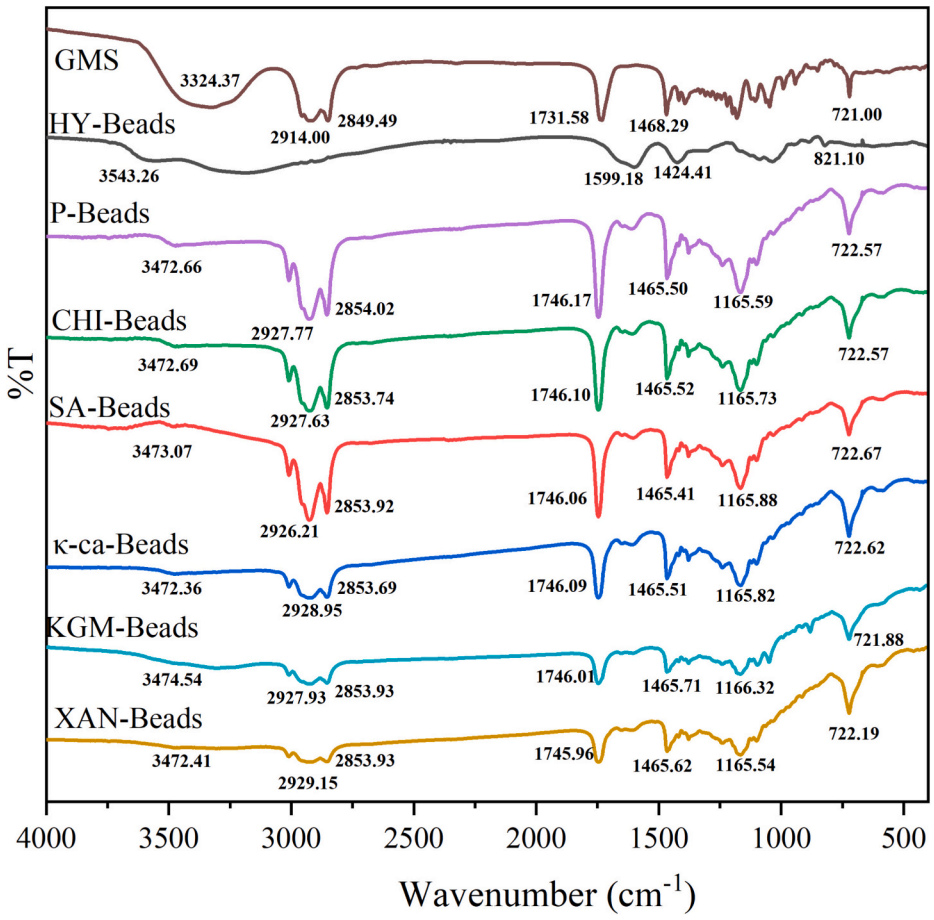

Fig. 3. FTIR spectra of bigel beads with different types of polysaccharides.

notable that bigel beads still kept intact structure in ESGF, probably because Na^+ ions seldom exchanged with Ca^{2+} ions in guluronic acid. The SA group changed in a relatively wider range than other groups. Regarding the roles of different polysaccharides, the gels containing xanthan gum and konjac gum didn't respond to Na^+ and exhibited the lowest swelling ratios. The swelling ratios of both beads grew rapidly to 1.09 in the initial 60 min, and decreased afterwards. After 180 min and 240 min, the swelling ratios reached equilibrium. The final swelling ratios were 1.15 and 1.16 for the XAN and KGM beads, respectively. A higher swelling ratio (~1.33) was seen in the CHI beads, which was attributed to the structural alterations of chitosan in low pH medium (Liu, 2018). In ESGF, the protonation of amino groups ($-NH^{3+}$) in chitosan molecules enhanced intermolecular repulsion, weakening the interaction between chitosan and alginate. Meanwhile, the increased hydrophilicity of chitosan chains further facilitated the penetration of water molecules, leading to a higher swelling ratio (Liu, 2018).

When the bigel beads were transferred into ESIF, rapid swelling occurred at the beginning, followed by slowed swelling until the gel beads ruptured and decomposed. This effect was the result of the deprotonation of the carboxyl groups on the alginate chains at neutral pH within the small intestine. As a result, the electrostatic repulsion between the alginate changes increases, resulting in swelling of the beads (Lin et al., 2024). Meanwhile, ion exchange occurred between Ca^{2+} and Na^+ to generate water-soluble alginate, causing structural damage to gel beads and eventually leading to the collapse of bead structures (Ramdhan et al., 2020). Fig. 5 illustrated that the inclusion of different polysaccharides could accelerate the swelling process of the beads to reach their maximum swelling ratios. The SA beads reached the highest swelling ratio (~2.27) at 180 min, whereas other beads reached the maximum swelling ratios at 120 min. For bigel beads with the same oleogel content, the alginate concentration in the aqueous phase significantly affected the swelling process in ESIF. The swelling rates of different bigel beads followed the order of CHI group ≈ KGM group > P group > XAN group > κ-ca group. It was noted that κ-car beads had similar swelling behavior in ESIF and ESGF in the first 120 min of digestion. The sulfate group in κ-carrageenan had a pKa of less than 2, suggesting that κ-carrageenan had a pH-independent swelling behavior (Joy, Vigneshkumar, John, & George, 2021). Furthermore, κ-carrageenan degraded slightly at acidic conditions, leading to an increase in pore size on the bead surface. On the contrary, in neutral environments, water penetration was inhibited, probably because of the formation of a more compact gel structure between κ-carrageenan and alginate (Li, Zhao, Sun, Yu, & Ma, 2019). The opposite swelling behaviors of κ-ca beads in ESGF and ESIF eventually masked the swelling responsiveness of the gel beads. Mahdavinia, Rahmani, Karami, and Pourjavadi (2014) also found that the pH-sensitivity of κ-carrageenan/alginate beads was reduced as the κ-carrageenan content increased.

3.6. Simulated gastrointestinal digestion of bigel beads

3.6.1. Structural changes of the bigel beads during digestion

CLSM was applied to observe the cross-section structures of bigel beads to evaluate the morphology and distribution of oleogel droplets (Fig. 6A). Before digestion, the oil droplets were packed tightly in the beads, and the green circle at the edge referred to the oil phase leaked from the beads. It was observed that the SA beads exhibited smaller oil droplets, and the droplets presented irregular shapes with slight coalescence. The morphology and distribution of oil droplets in the κ-ca and P beads were likewise comparable. The P beads had slightly larger oil droplet size than κ-ca beads. As compared to the SA beads, the CHI beads

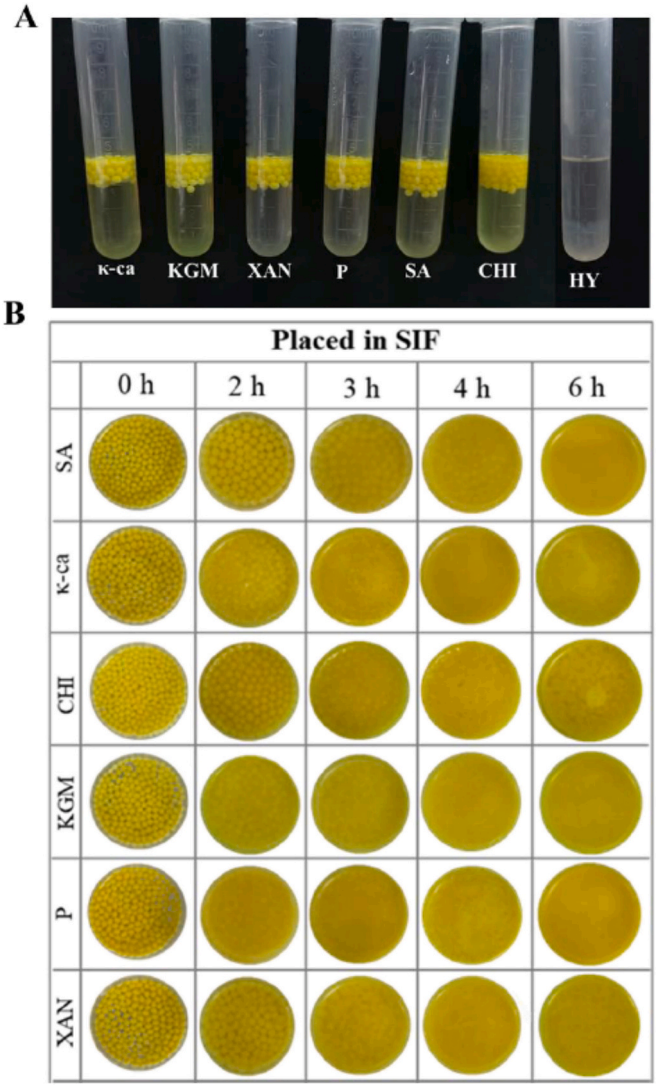

Fig. 4. Morphologies of bigel beads with different types of polysaccharides in ESGF (A) and ESIF (B).

showed a notable increase in oil droplet size, probably due to the low viscosity of the bigel emulsion before the formation of the beads. This finding was in agreement with previous researches. Behera, Sagiri, Singh, Pal, and Anis (2014) reported that droplet size of the dispersed phase in bigels rose as the viscosity of the continuous phase was decreased. In addition, a black layer was observed between the oil droplets at the edge of CHI beads and the surrounding green circles, which was probably from the coated chitosan layer on the bigel beads (indicated by the white arrows). The smallest oil droplets were found in the XAN and KGM groups as the emulsions had the highest viscosity, but the droplet boundary was blurred and clear coalescence was seen. Some black spherical region (water phase) was randomly distributed inside the oil droplets, suggesting the presence of some water-in-oil-in-water structures. In comparison to the XAN and KGM, pectin and κ-carrageenan could form double network structures within the alginate gels, and thus minimized oil droplet coalescence (Qi et al., 2020).

After SSF and SGF digestion, the highest hardness and the lowest ratio of hardness change (−0.060) were viewed in the SA beads, while the lowest hardness and the largest ratio of hardness change (−0.528) were observed in the κ-ca beads (Table 1). It was inferred that the bigel beads without polysaccharides were porous, and they were prone to form alginic acid skin and a denser structure in SGF. Morphologies of bigel beads at different stages of SIF digestion were shown in Fig. 6B, and the swelling capacity was influenced by the hardness and components of the beads. The SA beads presented the highest structural stability, which was consistent with the evolution of swelling behavior in ESIF. According to Fig. 6B, the spherical structure with a clear boundary was still visible in SA beads after 5 h of swelling in ESIF. This phenomenon could be explained by the high structural density and hardness of the SA beads, which was also observed in emulsion gel beads (Lin et al., 2022). At low pH, the hydrogen bonds between the carboxyl groups in alginate promoted densification of the gel structures, effectively inhibiting textural weakening caused by swelling (Ramdhan et al., 2020). After 3 h of SIF digestion, the bead size was decreased and the gel structure was disintegrated for the κ-ca, CHI and XAN bigel beads. After 4 h of SIF digestion, partial dissolution of KGM and P beads was observed. At the end of SIF digestion, no intact structure of the κ-ca, CHI and KGM beads could be observed, and some liquid oil appeared turned up at the surface, while some broken structures could still be found in the P and XAN beads. These findings revealed that the addition of polysaccharides accelerated the collapse of the gel structures in SIF. Fig. 6A showed that the SA beads maintained some of the gel structure with a large number of unevenly dispersed oil droplets inside, and the droplet size was remarkably larger than that in the original state. The results were attributed to the hydrolysis of fat by lipases, which in turn decreased the stability of droplets. Nevertheless, no bead structure of other bigel beads could be collected after the digestion. The digested liquids included a swarm of randomly distributed oil droplets of small size, revealing the decomposition of oil droplets by digestive enzymes.

It was worth mentioning that the SA and CHI bigel beads presented significantly different digestion behaviors, in comparison to the samples that did not experience gastric digestion (Fig. 4B). The SA beads kept their structure intact while the CHI beads presented rapid structural collapse. In an acidic environment, the chitosan coating of the CHI beads was swollen and disintegrated, which decreased their stability of beads in a neutral environment and caused rapid disintegration of their structure in SIF. When the CHI beads were incubated in ESIF, deprotonation of amino groups generated a denser exterior structure, which inhibited gel swelling and disintegration induced by electrostatic repulsion between deprotonated carboxyl groups in alginate molecules (Zhu et al., 2023). Furthermore, the formation of partially protonated carboxyl groups in SA during gastric digestion was responsible for the delayed structural collapse.

3.6.2. *In vitro release of EGCG*

Fig. 7A presents the release behavior of EGCG during SGF digestion. A faster release of EGCG was observed in all samples during the initial digestion in SGF for 20 min. Subsequently, the release rate of EGCG was decreased over time, and the ultimate cumulative release from different beads followed this order: P group (84.18 %) > κ-ca group (79.40 %) > CHI group (78.94 %) > SA group (65.72 %) > KGM group (57.24 %) > XAN group (41.75 %). A variety of factors could influence the release of EGCG, including the porosity of the gel network, the gel network relaxation and fragmentation (Yang et al., 2023). Qi et al. (2020) suggested that the inclusion of polysaccharides could affect the porosity of calcium alginate network in the dual network structures formed by pectin, carrageenan and alginate, and they found cavities in the gel structures. Therefore, the faster release of EGCG from P and κ-ca bigel beads was probably due to the decrease in density of the network structures. For CHI beads, the gel structures were relatively looser, as indicated by lower mechanical strength (Table 1). Moreover, the hydrophilicity of the chitosan layer was increased at acidic conditions and the interaction between the chitosan layer and the alginate was decreased, which could facilitate the diffusion of EGCG. The lower release in the KGM and XAN groups might be attributed to the high viscosity of the systems (Fig. 1), which hindered the mass transfer of EGCG. It was also observed that the XAN beads had the largest size, which was responsible for the delayed release of EGCG. As there was some water-in-oil-in-water structures in KGM and XAN bigel beads

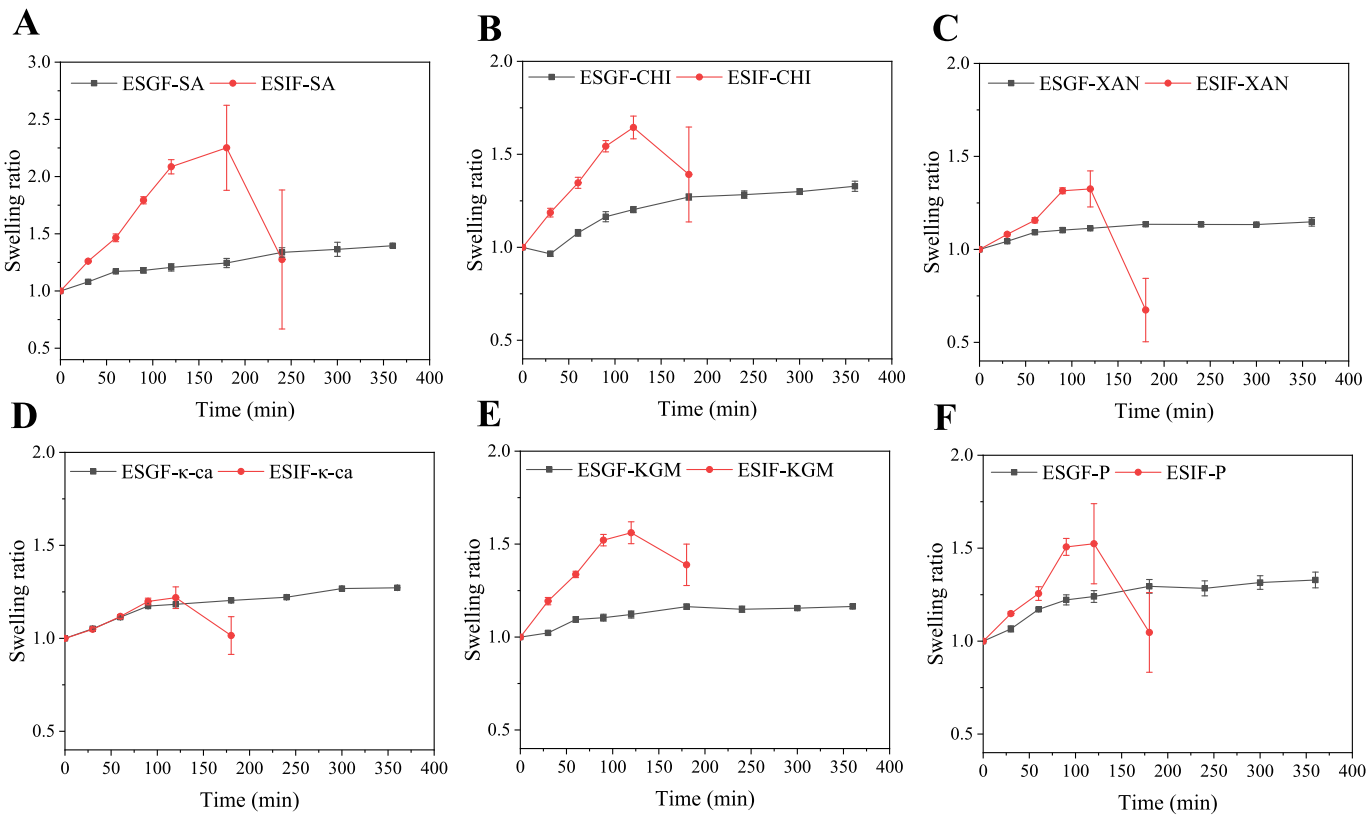

Fig. 5. Swelling degrees of different bigel beads in ESGF and ESIF. (A) SA group, (B) CHI group, (C) XAN group, (D) κ-ca group, (E) KGM group, and (F) P group.

(Fig. 6A), the release of water-soluble ingredients was thus delayed.

The release profile was analyzed by fitting the results of the curve to the different release kinetic models, and the fitting results were given in Table 2. It was seen that the release characteristics of the bigel beads during SGF digestion well fitted the Korsmeyer-Peppas model (R^2 values between 0.9882 and 0.9976). Therefore, the values of the release exponent (n) could help to identify the release mechanisms of EGCG from bigel beads. For a spherical delivery system, an "n" value <0.43 indicated Fickian diffusion of the bioactive (Ni, 2022). In the bigel beads containing polysaccharides, EGCG had an "n" value ranged from 0.25 to 0.3, suggesting the release of EGCG during SGF digestion followed Fickian diffusion, and the variation in polysaccharide types did alter this mechanism.

3.6.3. *In vitro release of curcumin*

The release profile of curcumin in bigel beads during simulated gastrointestinal digestion was also determined (Fig. 7B). Only minor curcumin was released (<0.35 %) after SGF digestion, as curcumin was mainly present in the oleogel phase, which closely filled in the pores of the alginate network. Network relaxation during SGF swelling was limited, and thus the internal leakage of oil droplets was inhibited. As a result, only part of the curcumin present in the micelles diffused out of the network structure with a very limited release. These findings suggested that the bigel beads could effectively reduce the loss of curcumin during SGF digestion, allowing more curcumin to be released in small intestine. Similar findings were also reported in emulsion gels, bigel emulsions (Mao et al., 2020). In a previous study, the modification of the interfacial structures did not increase the release of curcumin in SGF, highlighting the strong barrier effect of the alginate gel structures (Zhang et al., 2025).

When transferred to SIF, the release profile of curcumin from all bigel bead showed sharp increase at the beginning and continued to grow over time. The findings were in agreement with literature studies on protein based bigel beads (Lin et al., 2024). The ultimate cumulative release of curcumin from different bigel beads followed the order of P group > κ-ca group > CHI group > XAN group > KGM group > SA group. In the SA group, the release rate of curcumin was decreased between 360 and 480 min. The release rate grew again once the release percentage reached 15.65 %, and the release amount reached its maximum of 33.98 %. Similar trends were observed in the P and κ-ca groups, with the maximum release percentage of 48.29 % and 46.65 %, respectively. The CHI, XAN, and KGM groups, on the other hand, maintained high release rates, with the final release percentage of 41.24 %, 38.95 %, and 37.77 %, respectively. Lipid digestion took place when the pancreatic lipase was adsorbed onto the oil-water interface and contacted with the substrate (such as triglycerides, diglycerides, etc.), which would facilitate curcumin release during SIF digestion. In the case of bigels, pancreatic lipase must diffuse into hydrogel network before reaching the oil droplet. When the bigel beads transferred into SIF, the rapid swelling of the gel structure enlarged network pore size, allowing the easier access of lipase into the interior of the bigels and digestion of the oil phase. As a result, fast curcumin release was observed. With further swelling, the exterior gel structures would collapse, and fragmentation of the gel structure resulted in the release of oil droplets, allowing further contact between oil droplets and pancreatic lipase. Previous studies indicated that the rate and extent of oil phase digestion were related to the pore size of alginate gel network, gel bead size and oil droplet size (Rungraung et al., 2022). For the SA group, the presence of a strong gel network structure hindered the diffusion of pancreatic lipase molecules into the gel network. Furthermore, the beads retained a relatively intact structure throughout the SIF digestion, reducing oleogel release and further digestion. On the other hand, the curcumin release was affected by free fatty acids on the droplet surface. To remove free fatty acids from the surface and promote oleogel digestion, the fatty acids were usually absorbed into mixed micelles composed of bile salts and phospholipids, or form insoluble salts with calcium ions (Devraj et al., 2013). Therefore, the relatively compact network in the SA beads hindered the diffusion of bile salts, phospholipids and other substances,

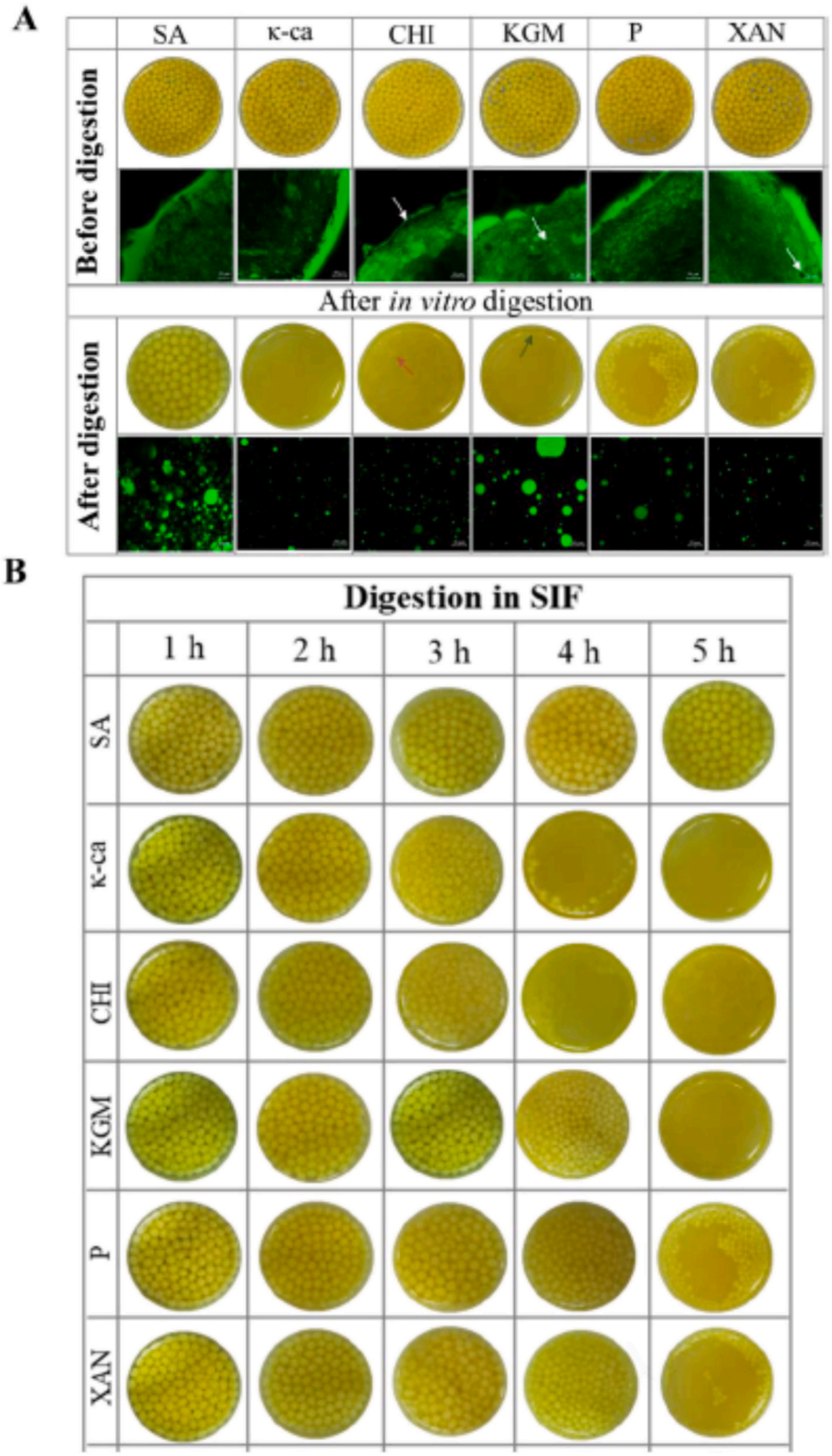

Fig. 6. CLSM images of fresh bigel beads and bigel beads after in vitro digestion (A); Morphologies of bigel beads at different times during digestion in SIF (B).

attributing to the delay of curcumin release (Zhang et al., 2016). Notably, the SA beads showed the highest swelling ratio in SIF (Fig. 6), suggesting the swelling ratio an indecisive factor on the release of curcumin. The rapid dissolution of bigel beads combined with polysaccharides in SIF aided lipase digestion and bioactive release, leading to a higher release percentage. For the gel beads containing polysaccharide, the microstructure images revealed significant oil droplet coalescence in the CHI, XAN and KGM groups, which resulted in a limited contact area between oil droplets and pancreatic lipase and delayed lipid digestion and curcumin release (Torcello-Gómez & Foster, 2017).

To further investigate the release kinetics of curcumin from the bigel

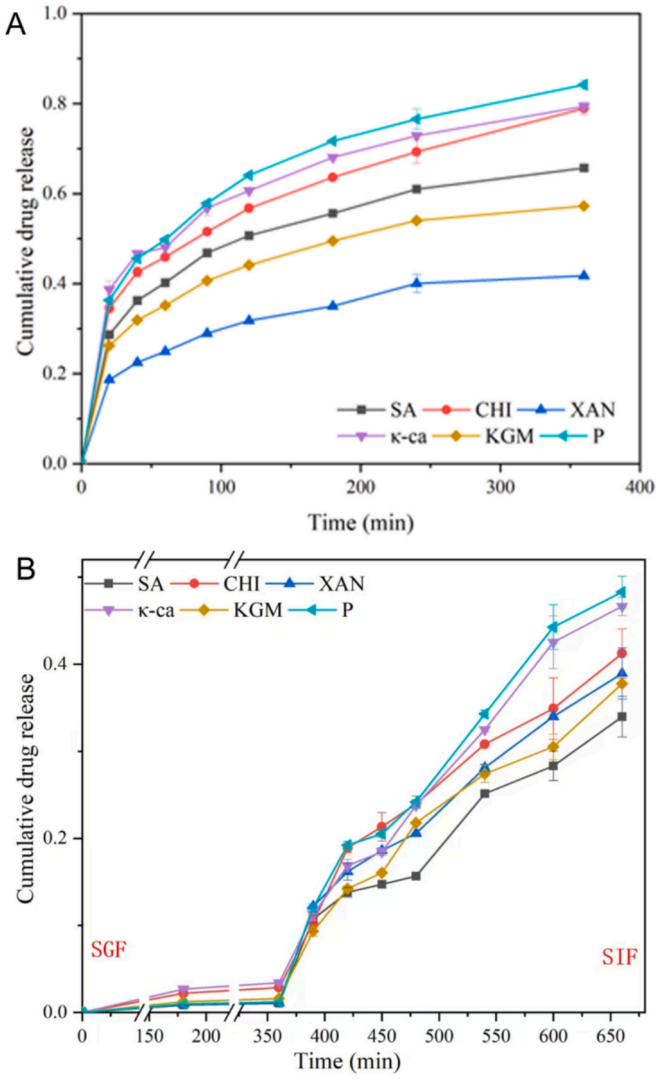

Fig. 7. EGCG (A) and curcumin (B) release curve in bigel beads with different types of polysaccharides.

beads, different models were used to fit the results (Table 2). The release of curcumin during SIF digestion was found to follow Korsmeyer-Peppas model (R^2 values between 0.9507 and 0.9884) and Higuchi kinetics model (R^2 values between 0.9458 and 0.9841). The n values of all bigel beads ranged from 0.5419 to 0.6926, suggesting that the release of curcumin followed a non-Fickian diffusion, which was controlled by both diffusion and dissolution of the systems.

4. Conclusion

In this work, we developed novel bigel beads based on alginate hydrogel and GMS oleogels, and different types of polysaccharides were added to adjust the structures and functions of the beads. The tested polysaccharides were able to reduce the hardness of the beads, and facilitate the beads to resist shrinking during gelation and also swelling in simulated gastric and intestinal fluid. The bigel beads were able to co-deliver lipophilic and hydrophilic bioactives simultaneously, and the bead structure significantly affected the release of EGCG and curcumin during gastric and intestinal digestion. Among all tested bigel beads, the P and κ-ca beads exhibited the highest cumulative drug release in SIF, which was favored for the development of functional food. The release kinetics of EGCG and curcumin followed Fickian and non-Fickian diffusion, which was not affected by the type of added polysaccharide. Therefore, this study offered new insights regarding the structure-function relationship of bigel beads. In the future, the beads could be incorporated into complex food systems, e.g., candy, yoghurt, beverages, to test their functional properties. The information obtained in this study showed that bigel beads had great potential as delivery systems for the development of functional food.

Funding

This work was supported by the Collaborative Innovation Center of the Beijing Academy of Agriculture and Forestry Sciences (Grant No. KJCX20240402), the Innovation and Capacity-Building Project by the Beijing Academy of Agriculture and Forestry Sciences (Grant No. KJCX20240331, KJCX20230212).

CRediT authorship contribution statement

Guangmin Liu: Writing – original draft, Investigation. **Yuxuan Wang:** Investigation. **Jingyi Yang:** Investigation. **Yaqin Wang:** Writing – review & editing, Formal analysis. **Hongju He:** Supervision, Conceptualization. **Like Mao:** Writing – original draft, Methodology.

Declaration of competing interest

The authors declare that they have no known competing financial interests or personal relationships that could have appeared to influence the work reported in this paper.

Table 2
The kinetic parameters of the EGCG and curcumin released from different bigel beads.

Compound	Samples	Zero-order kinetics model	First-order kinetics model	Hixson-Crowell model	Higuchi kinetics model	Korsmeyer-Peppas model		
		R^2	R^2	R^2	R^2	k	n	R^2
EGCG	SA	0.6872	0.7999	0.3467	0.9187	0.1297	0.2800	0.9928
	CHI	0.7218	0.8770	0.3541	0.9324	0.1436	0.2878	0.9976
	XAN	0.7049	0.8301	0.3540	0.9269	0.0783	0.2894	0.9882
	κ-ca	0.6637	0.8492	0.3295	0.8991	0.1784	0.2553	0.9926
	KGM	0.6821	0.8179	0.3428	0.9148	0.1170	0.2746	0.9923
	P	0.7036	0.8172	0.3536	0.9278	0.1569	0.2887	0.9946
curcumin	SA	0.9504	0.9653	0.7504	0.9585	0.0108	0.5996	0.9507
	CHI	0.9448	0.8514	0.7918	0.9841	0.0184	0.5419	0.9884
	XAN	0.9524	0.9662	0.7327	0.9836	0.0151	0.5660	0.9827
	κ-ca	0.9852	0.9468	0.8870	0.9458	0.0091	0.6926	0.9858
	KGM	0.9635	0.9123	0.7980	0.9756	0.0110	0.6150	0.9883
	P	0.9680	0.9366	0.7778	0.9663	0.0116	0.6561	0.9811

Appendix A. Supplementary data

Supplementary data to this article can be found online at https://doi.org/10.1016/j.fochx.2025.102359.

Data availability

Data will be made available on request.

References

Al-Faken, M. S., Al-Subaie, N. S., EL-Ghoul, Y., & Hamden, Z. (2024). Preparation and properties of a novel alginate/carrageenan crosslinked coordination polymer and evaluation of the antibacterial, antioxidant and anticancer potential of its co(ii), and Cr(iii) polymeric complexes. *RSC Advances, 14*, 38934–38943. https://doi.org/10.1039/d4ra06818a

Aw, Y. Z., Lim, H. P., Low, L., Goh, B., Chan, E., & Tey, B. (2023). Pickering emulsion hydrogel beads for curcumin encapsulation and food application. *Journal of Food Engineering, 350*, Article 111501. https://doi.org/10.1016/j.jfoodeng.2023.111501

Behera, B., Sagiri, S. S., Singh, V. K., Pal, K., & Anis, A. (2014). Mechanical properties and delivery of drug/probiotics from starch and non-starch based novel bigels: A comparative study. *Starch-starke, 66*, 865–879. https://doi.org/10.1002/star.201400045

Belščak-Cvitanović, A., Komes, D., Karlović, S., Djaković, S., Špoljarić, I., Mršić, G., & Ježek, D. (2015). Improving the controlled delivery formulations of caffeine in alginate hydrogel beads combined with pectin, carrageenan, chitosan and psyllium. *Food Chemistry, 167*, 378–386. https://doi.org/10.1016/j.foodchem.2014.07.011

Berninger, T., Mitter, B., & Preininger, C. (2016). The smaller, the better? The size effect of alginate beads carrying plant growth-promoting bacteria for seed coating. *Journal of Microencapsulation, 33*(2), 127–136. https://doi.org/10.3109/02652048.2015.1134690

Cao, L., Lu, W., Mata, A., Nishinari, K., & Fang, Y. (2020). Egg-box model-based gelation of alginate and pectin: A review. *Carbohydrate Polymers, 242*, Article 116389. https://doi.org/10.1016/j.carbpol.2020.116389

Chung, S. S., & Vadgama, J. V. (2015). Curcumin and epigallocatechin gallate inhibit the cancer stem cell phenotype via down-regulation of STAT3-NFκB signaling. *Anticancer Research, 35*, 39–46.

Cofelice, M., Messia, M. S., Marconi, E., Cuomo, F., & Lopez, F. (2023). Effect of the xanthan gum on the rheological properties of alginate hydrogels. *Food Hydrocolloids, 142*, Article 108768. https://doi.org/10.1016/j.foodhyd.2023.108768

Cui, C., Jiang, H., Guan, M., Ji, N., Xiong, L., & Sun, Q. (2022). Characterization and in vitro digestibility of potato starch encapsulated in calcium alginate beads. *Food Hydrocolloids, 126*, Article 107458. https://doi.org/10.1016/j.foodhyd.2021.107458

Dashevsky, A. (1998). Protein loss by the microencapsulation of an enzyme (lactase) in alginate beads. *International Journal of Pharmaceutics, 161*(1), 1–5. https://doi.org/10.1016/S0378-5173(97)00172-5

Devraj, R., Williams, H. D., Warren, D. B., Mullertz, A., Porter, C. J. H., & Pouton, C. W. (2013). In vitro digestion testing of lipid-based delivery systems: Calcium ions combine with fatty acids liberated from triglyceride rich lipid solutions to form soaps and reduce the solubilization capacity of colloidal digestion products. *International Journal of Pharmaceutics, 441*(1), 323–333. https://doi.org/10.1016/j.ijpharm.2012.11.024

Goodacre, R., & Anklam, E. (2001). Fourier transform infrared spectroscopy and chemometrics as a tool for the rapid detection of other vegetable fats mixed in cocoa butter. *Journal of the American Oil Chemists' Society, 78*, 993–1000. https://doi.org/10.1007/s11746-001-0377-x

Joy, R. J., Vigneshkumar, P. N., John, F., & George, J. (2021). Hydrogels based on carrageenan. In *Plant and Algal Hydrogels for Drug Delivery and Regenerative Medicine*, ed. Giri, T. K., Ghosh, B. pp293–325. Woodhead Publishing: Cambridge, England.

Kour, P., Afzal, S., Gani, A., Zargar, M. I., Tak, U. N., Rashid, S., & Dar, A. A. (2022). Effect of nanoemulsion-loaded hybrid biopolymeric hydrogel beads on the release kinetics, antioxidant potential and antibacterial activity of encapsulated curcumin. *Food Chemistry, 376*, Article 131925. https://doi.org/10.1016/j.foodchem.2021.131925

Lee, B. B., Ravindra, P., & Chan, E. (2013). Size and shape of calcium alginate beads produced by extrusion dripping. *Chemical Engineering & Technology, 36*(10), 1627–1642. https://doi.org/10.1002/ceat.201300230

Li, J. Y. (2019). *Encapsulation of IgY by sodium alginate-based composite hydrogels and study on its release properties.* Jiangnan University (MA thesis.).

Li, L., Zhao, J., Sun, Y., Yu, F., & Ma, J. (2019). Ionically cross-linked sodium alginate/κ-carrageenan double-network gel beads with low-swelling, enhanced mechanical properties, and excellent adsorption performance. *Chemical Engineering Journal, 372*, 1091–1103. https://doi.org/10.1016/J.CEJ.2019.05.007

Li, Y., Fan, R., Xing, H., Fei, Y., Cheng, J., & Lu, L. (2021). Study on swelling and drug releasing behaviors of ibuprofen-loaded bimetallic alginate aerogel beads with pH-responsive performance. *Colloids and Surfaces B: Biointerfaces, 205*, Article 111895. https://doi.org/10.1016/j.colsurfb.2021.111895

Lin, D., Kelly, A. L., Maidannyk, V., & Miao, S. (2021). Effect of structuring emulsion gels by whey or soy protein isolate on the structure, mechanical properties, and in-vitro digestion of alginate-based emulsion gel beads. *Food Hydrocolloids, 110*, Article 106165. https://doi.org/10.1016/j.foodhyd.2020.106165

Lin, D., Kelly, A. L., & Miao, S. (2022). The impact of pH on mechanical properties, storage stability and digestion of alginate-based and soy protein isolate-stabilized emulsion gel beads with encapsulated lycopene. *Food Chemistry, 372*, Article 131262. https://doi.org/10.1016/j.foodchem.2021.131262

Lin, Q., Li, X., McClements, D. J., Jin, Z., Qiu, C., & Li, G. (2024). Plant-based delivery systems for controlled release of hydrophilic and hydrophobic active ingredients: Pea protein-alginate bigel beads. *Food Hydrocolloids, 154*, Article 110101. https://doi.org/10.1016/j.foodhyd.2024.110101

Liu, C. (2018). *Preparation of pH sensitive chitosan hydrogel microspheres for controlled drug delivery*. Zhejiang Ocean University (MA thesis.).

Mahdavinia, G. R., Rahmani, Z., Karami, S., & Pourjavadi, A. (2014). Magnetic/pH-sensitive κ- carrageenan/sodium alginate hydrogel nanocomposite beads: Preparation, swelling behavior, and drug delivery. *Journal of Biomaterials Science Polymer Edition, 25*(17), 1891–1906. https://doi.org/10.1080/09205063.2014.956166

Mao, L., Lu, Y., Cui, M., Song, M., & Gao, Y. (2020). Design of gel structures in water and oil phases for improved delivery of bioactive food ingredients. *Critical Reviews in Food Science and Nutrition, 60*(10), 1651–1666. https://doi.org/10.1080/10408398.2019.1587737

Murata, Y., Sasaki, N., Miyamoto, E., & Kawashima, S. (2000). Use of floating alginate gel beads for stomach-specific drug delivery. *European Journal of Pharmaceutics and Biopharmaceutics, 50*(2), 221–226. https://doi.org/10.1016/S0939-6411(00)00110-7

Ni, F. F. (2022). Study on the co-encapsulation of lactobacillus plantarum and curcumin by alginate-gelatin hydrogel beads. *Zhejiang Gongshang University.*. https://doi.org/10.27462/d.cnki.ghzhc.2022.000810

Qi, X., Simsek, S., Chen, B., & Rao, J. (2020). Alginate-based double-network hydrogel improves the viability of encapsulated probiotics during simulated sequential gastrointestinal digestion: Effect of biopolymer type and concentrations. *International Journal of Biological Macromolecules, 165*, 1675–1685. https://doi.org/10.1016/j.ijbiomac.2020.10.028

Ramdhan, T., Ching, S. H., Prakash, S., & Bhandari, B. (2020). Physical and mechanical properties of alginate based composite gels. *Trends in Food Science & Technology, 106*, 150–159. https://doi.org/10.1016/j.tifs.2020.10.002

Rungraung, N., Jain, S., Mitbumrung, W., Khomein, P., Suphantharika, M., McClements, D. J., & Winuprasith, T. (2022). Controlling the in vitro gastrointestinal digestion of emulsified lipids by encapsulation within nanocellulose-fortified alginate beads. *Food Structure, 32*, Article 100266. https://doi.org/10.1016/j.foostr.2022.100266

Shakeel, A., Farooq, U., Iqbal, T., Yasin, S., Lupi, F. R., & Gabriele, D. (2019). Key characteristics and modelling of bigels systems: A review. *Materials Science and Engineering C, 97*, 932–953. https://doi.org/10.1016/j.msec.2018.12.075

Torcello-Gómez, A., & Foster, T. J. (2017). Instant polysaccharide-based emulsions: Impact of microstructure on lipolysis. *Food & Function, 8*(6), 2231–2242. https://doi.org/10.1039/c7fo00536a

Wu, B., Li, H., Xia, Q., & Li, Y. (2022). The influence of Ca^{2+}/K^{+} weight ratio on the physicochemical properties and in vitro digestion behavior of resveratrol-loaded Pickering emulsions encapsulated in alginate/κ-carrageenan hydrogel beads. *Reactive and Functional Polymers, 181*, Article 105414. https://doi.org/10.1016/j.reactfunctpolym.2022.105414

Wu, B., Li, Y., Li, Y., Li, H., Li, L., & Xia, Q. (2022). Encapsulation of resveratrol-loaded Pickering emulsions in alginate/pectin hydrogel beads: Improved stability and modification of digestive behavior in the gastrointestinal tract. *International Journal of Biological Macromolecules, 222*, 337–347. https://doi.org/10.1016/j.ijbiomac.2022.09.175

Yang, J., Song, J., Miao, S., Gao, Y., & Mao, L. (2024). Alginate-based gel beads with bigel structures: Preparation, characterization and bioactive encapsulation. *Food Hydrocolloids, 146*, Article 109294. https://doi.org/10.1016/j.foodhyd.2023.109294

Yang, Z., McClements, D. J., Li, C., Sang, S., Chen, L., Long, J., … Jin, Z. (2023). Targeted delivery of hydrogels in human gastrointestinal tract: A review. *Food Hydrocolloids, 134*, Article 108013. https://doi.org/10.1016/j.foodhyd.2022.108013

Zhang, F., Mao, P., Kong, H. L., Zhao, M., Fang, Y. P., Nishinari, K., & Phillips, G. O. (2013). Critical behavior of gelation of alginate/xanthan mixtures induced by Ca^{2+} ions. *Acta Polymerica Sinica, 11*, 1390–1398. https://doi.org/10.3724/SP.J.1105.2013.13071

Zhang, R., Yang, J., Li, J., Gao, Y., & Mao.. (2025). Modification of the interface of oleogel-hydrogel bigel beads for enhanced stability and prolonged release of bioactives. *Food Chemistry, 468*, Article 142448. https://doi.org/10.1016/j.foodchem.2024

Zhang, Z., Zhang, R., Zou, L., Chen, L., Ahmed, Y., Al Bishri, W., … McClements, D. J. (2016). Encapsulation of curcumin in polysaccharide-based hydrogel beads: Impact of bead type on lipid digestion and curcumin bioaccessibility. *Food Hydrocolloids, 58*, 160–170. https://doi.org/10.1016/j.foodhyd.2016.02.036

Zheng, H., Mao, L., Cui, M., Liu, J., & Gao, Y. (2020). Development of food-grade bigels based on κ-carrageenan hydrogel and monoglyceride oleogels as carriers for *β*-carotene: Roles of oleogel fraction. *Food Hydrocolloids, 105*, Article 105855. https://doi.org/10.1016/j.foodhyd.2020.105855

Zhu, Z., Yuan, Y., Guo, J., Luo, X., Liu, S., & Miao, S. (2023). Encapsulation of SOD in chitosan-coated gel particles of alginate or mixture of alginate and shellac for targeted intestinal delivery. *Food Hydrocolloids, 142*, Article 108778. https://doi.org/10.1016/j.foodhyd.2023.108778